Measurement of Mechanical Properties Using Slender Cantilever Beams

L.J. Vandeperre[+‡], X. Wang[+*] and A. Atkinson[+]

[+]Department of Materials, Imperial College London, South Kensington Campus, London SW7 2AZ, UK

‡ Centre for Advanced Structural Ceramics, Imperial College London, South Kensington Campus, London SW7 2AZ, UK

Abstract

The measurement of mechanical properties of materials only available in the form of thin sheets requires the use of load cells and displacement sensors of high sensitivity at low applied loads. These are available in testing platforms such as instrumented nano-indenters. In the current work, the elastic modulus and fracture toughness of thin cantilever beams of a representative brittle thin sheet material (300 μm thick NiO/YSZ support for a solid oxide fuel cell) were measured using a micro-/nano-indenter. The Young's modulus and K_{IC} were determined to be 139±4 GPa and 2.13±0.27 MPa $m^{0.5}$ respectively using this method.

Keywords: Fracture toughness; Cantilever beams; Solid oxide fuel cells; Anode; Nano-indenter

I Introduction

Solid oxide fuel cells (SOFCs) have ceramic or ceramic containing materials as the key components, such as electrolyte and electrodes, which allow SOFCs to operate at elevated temperatures for converting chemical energy directly into electricity with a high efficiency. Since ceramics are intrinsically brittle, mechanical failure by fracture can occur in these key SOFC components under the influence of mechanical and/or thermal stresses in the stack. Mechanical failure could lead to lowered performance and shortened lifetime of SOFCs [1-3]. Therefore knowledge of the mechanical properties of these key components is essential for developing high performance SOFCs with prolonged lifetime.

* Tel: +44 20 75496809, Fax:+44 20 75946757,
E-mail address: xin.wang@imperial.ac.uk

Fracture toughness in mode I (K_{IC}) is a fundamental parameter, which measures the resistance to cracking or breaking for a material. Prediction of crack growth during service requires the accurate determination of the properties of the materials and of interfaces between materials. Where such materials exist in bulk, a wide range of established methods can be used to determine these properties, but in the case of SOFCs some materials only exist in the form of relatively thin layers or sheets. For example, the electrolyte and electrodes in SOFCs can be as thin as a few microns. This is a challenge because the force needed to deform such thin specimens is very low and carrying out such experiments therefore requires sensitive load cells and accurate displacement measurements typically not achieved by standard test frames.

However, with the advent of instrumented indenters, mechanical test benches capable of applying small loads (μN-N) and measuring displacements with a resolution of the order of nano-meters have become available. The aim of this work was therefore to define a protocol for measuring the stiffness and toughness of thin specimens using the high load and displacement resolution of a nano- or micro-indenter. Because of the arrangement of our system, in which the indenter is a pendulum and moves along a horizontal axis, the specimen must be fixed in a vertical orientation, see Fig.1. This precludes the use of a horizontal 3 point bending method as the sample would slide off the supports. However, it is appropriate for a cantilever beam as this requires the clamping of the specimen in position for the test.

II Experimental

2.1 Specimens

The specimens were thin beams of NiO/3YSZ (3YSZ indicates ZrO_2 doped with 3 mol% Y_2O_3) composite typical of an anode support for a SOFC in its oxidised state. The beams were laser machined from a larger sheet and had nominal dimensions 20 mm by 3 mm by 0.3 mm. The porosity of the specimens was measured to be 16.2±0.1%.

The elastic modulus of glass microscope slides was also measured in order to verify the clamping method.

2.2 Notch making for toughness measurement

To measure the fracture toughness, a V-shaped sharp notch needs to be introduced on one side of the beam [4]. Due to the small thickness and brittle nature of the specimens, a normal diamond wheel is not suitable for creating the required notch geometry. In this work, the notch was made manually using a sharp steel knife moving in a precision guide block. The knife was lubricated with diamond suspension (0.3 μm) so that fine particles of diamond carried on the knife edge would erode the material and produce a sharp tip to the notch. The actual notch profile was characterised using a surface profilometer (Dektak 150, Veeco Instruments) and an example profile is shown in Fig. 2. The notch was roughly V-shape, with notch width at opening (NW) typically equal to or slightly smaller than the notch depth *a*: i.e. $0.8a < NW < a$. Microscopic examination of the notch tip revealed the notch tip width was typically in the range 5 to 10μm.

For accurate determination of K_{IC}, the notch depth needs be measured accurately. For these specimens, this was done by optical microscopic examination of the fractured cross section of the specimen (Fig. 2b). Due to the grinding process during notch making, its lighter grey surface was easily distinguishable from the freshly fractured surface which had the characteristic green colour of the non-reduced anode support (the colour of NiO). The notch depth was then measured by image analysis using ImageJ software.

2.3 Specimen clamping and bending test

For the mechanical test on the cantilever beam, the clamping of the end of the beam needs to be sufficiently rigid to obtain a known stress distribution at the notch for fracture toughness measurement and to describe the load versus displacement using beam theory when measuring elastic modulus with an un-notched sample. On the other hand, due to the brittle nature of the test material, the sample holder should avoid loading the clamped material irregularly. Therefore a suitable clamping arrangement was designed as shown in Fig. 3, in which a depression equal to the thickness of the specimen (300 μm for the composite specimens) was left between the top and bottom parts of the clamp over half the width of the clamp. This also provided a guide to align the beam for testing. A thin layer of isocyanate adhesive was applied to the bottom of the depression to spread the load on the sample over any deviation from flatness and to enhance the rigidity of the clamp. The sample clamping was finally secured using screws between the top and bottom parts of the clamp. For measurement of the fracture toughness, the distance from the clamping edge to the notch tip is denoted as *ND* and the distance from the loading point to the notch is *L*. The indenter platform has restrictions on the upper bounds of both loading (< 20 N) and displacement (<

50 µm). A spherical sapphire indenter tip with a diameter of 500 µm was used for applying the load to the cantilever beam on the centre line of its upper face.

III Results and discussion

3.1 Experimental validation of the set-up

Stiffness measurements were carried out on glass strips to validate the method of loading and clamping. The dimensions and elastic modulus (determined independently using the impulse excitation of vibration (or resonance) method [5]) of these samples are shown in Table 1.

The procedure consisted of measuring the load-displacement relation for the beam by allowing the indenter to move 50 µm, which is the maximum allowed displacement of the machine, followed by unloading to 20% of the maximum load and re-loading 4 times before final complete unloading. Then the indenter was moved along the length of the beam by 1 or 2 mm and the experiment repeated so that a range of curves as a function of beam length were obtained. Fig. 4 shows an example of the load-displacement curves obtained for the glass sample, when it was loaded at 4 mm from the clamped end.

The slope of each of the loading and unloading curves in Fig. 4 was determined, and the average of these was taken as the stiffness of the beam. It is clear that the slope is highly repeatable. The average stiffness of the cantilever during loading was 5880 ± 45 N/m, slightly lower than that during unloading (5927 ± 27 N/m). For this example the overall average was 5903 N/m and the standard deviation was 0.69% of the average value.

Fig. 5 shows the stiffness as a function of the distance between the clamped end and the loading point for the glass sample. Since the stiffness is proportional to $1/L^3$, the stiffness increases dramatically as the distance becomes shorter. The predicted lines are the stiffness values calculated using the independently measured elastic modulus of the sample using the resonance method given in Table 1. Fig. 5 clearly shows a good agreement between the prediction and measurement.

In addition, since a point load via spherical indenter was used, it is important to check how much the results could be influenced by the loading point not being on the centre line of the beam. This was checked by both experiments and FE modelling. It was found that when the loading point was offset from the centre line by 1 mm on a 3 mm wide beam, the error was less than 5%. Therefore, the error from the loading point deviating from centre line is negligible (since the maximum potential error in the loading point was found to be < 0.2 mm).

The relationship between stiffness and Young's modulus can be expressed as:

$$S = \frac{Ewt^3}{4L^3} \qquad \text{Eq. 1}$$

where *w* is the beam width, *t* beam thickness and *E* is Young's modulus. Based on the data in Fig. 5, the average Young's modulus of the glass can be calculated as 79 ±11GPa, which is ~ 10% deviated from the value determined by resonance method (given in Table 1). Therefore it can be concluded that accurate measurements of beam deflection and load can be made for thin specimens such that the Young modulus of the materials can be measured.

3.2 Young's modulus of anode support specimens

Anode specimens were found to have good consistency of elastic modulus from specimen to specimen. As shown in Fig. 6 the loading-unloading curves for two different NiO/YSZ specimens are very close and the average stiffness, *S*, is 1.1×10^4 N/m. The Young's modulus of the specimens was measured to be 139±4 GPa using the cantilever beam method in good agreement with the value of 136 ± 6 GPa using the resonance method.

3.3 Fracture toughness of the anode support specimens

Notched cantilever beams have been reported in the literature for stress-corrosion cracking studies and fracture testing of weldments [6, 7]. A semi-empirical relationship between the applied load and the stress intensity at the crack (notch) tip was given as [6, 7]:

$$\mathrm{K}_{Ic} = \frac{4.12\mathrm{FL}}{\mathrm{wt}^{1.5}}\left[\frac{1}{(1-\frac{\mathrm{a}}{\mathrm{t}})^3} - (1-\frac{\mathrm{a}}{\mathrm{t}})^3\right]^{0.5} \qquad \text{Eq. 2}$$

where the coefficient 4.12 was obtained by fitting to calibration data [6], *F* is the applied load.

Eq.2 was obtained by extending a solution for a deep notch by adding the second term in the bracket in order to adapt it to both shallow and deep notches and was verified with calibration data [6]. Therefore Eq.2 is a semi-empirical equation. Recently we derived an equation based on a clearer physical model and more rigorous derivation for plane strain conditions [8]:

$$K_{Ic} = \sqrt{\frac{6}{(1-\nu^2)}\frac{FL}{wt^{1.5}}\left[\frac{2}{(1-\frac{a}{t})^3} + \frac{(1-\frac{t}{L})}{(1-\frac{a}{t})^2}\right]^{0.5}} \qquad \text{Eq. 3}$$

where ν is Poisson's ratio, and all other symbols have the same meaning as those in Eq.2. Unlike Eq.2, Eq.3 shows that K_{IC} depends not only on the ratio *a/t* but also on *t/L*. The term $(1-\nu^2)$ in Eq.3 comes from the plane strain assumption in the derivation. In a separate paper [8] it has been shown that Eq.2 shows good numerical agreement with Eq.3 in typical cases, despite the differences in functional form. Nevertheless, in this work both equations were used and compared.

A typical load-displacement curve obtained on the micro-indentation platform with a notched NiO/YSZ anode support specimen is shown in Fig. 7, and is linear up to the fracture point. The data beyond the fracture point in Fig. 7 are artefacts due to the maximum measureable displacement of the instrument which is 50 µm. Any displacement larger than the maximum is recorded as being the maximum measurable.

The beam compliance is dependent on the notch depth and can be represented as:

$$C = (h+\Delta h)/F \qquad \text{Eq. 4}$$

where *h* is the displacement at the loading point in the absence of the notch and is given by:

$$h = \frac{4F(L+Nd)^3}{Ewt^3} \qquad \text{Eq. 5}$$

and Δh is the additional displacement at the loading point due to the presence of the notch, which according to [8] is given by:

$$\Delta h = \frac{12FL}{Ew}\left\{\frac{[a(L+t)-t^2]\boldsymbol{t}}{a^2(\boldsymbol{t}-a)^2} + \frac{at-aL+t^2}{a^2t}\right\} - \frac{12FL(2Lt-t^2)}{Ewt^3} \qquad \text{Eq. 6}$$

For slender specimens, *L* >> *t*, therefore the expression for compliance can be simplified as:

$$C = \frac{4}{Ewt^3}\left[(L+ND)^3 - 6tL^2 + \frac{3aL^2(2-\gamma)}{\gamma(1-\gamma)^2}\right] \qquad \text{Eq. 7}$$

where $\boldsymbol{\gamma = a/t}$.

Fig. 7 shows the prediction of Eq. 7, using the previously measured value for *E* and the notch depth measured by optical microscopy after fracture. The compliance predicted by Eq. 7 is 23.3 µm/N which is in good agreement with the experimental result of 22.8 µm/N. Therefore the high resolution load-displacement data may be used to check the test condition, or conversely to estimate the notch depth non-destructively. Fig. 8 shows an example of the strong dependence of the compliance on the notch depth: a small change in notch depth (e.g. by 5 μm) can lead to noticeable changes in the compliance. This means the crack length (or notch depth) can be estimated using Eq.7 if other techniques are either unavailable or are judged to be unreliable.

Table 2 lists the values of K_{IC} measured under different conditions for the anode support samples. Despite the variability in experimental conditions (especially in notch depth), only a small scatter exists in the measured values. The good repeatability of the results indicates that the cantilever beam method is a robust method for testing slender specimens. In addition, it is interesting to note that the mean values of K_{IC} calculated using the two different equations (2 and 3) agree with each other very well, although the two equations give slightly different results on individual specimens

Fig. 9 plots the measured K_{IC} against the relative notch depth a/t. There is no distinguishable dependence of the measured K_{IC} on notch depth. However it is clear that Eq.3 and Eq.2 agree best within the range of a/t = 0.4-0.6. When $a/t < 0.4$, Eq.3 gives higher K_{IC} values than those calculated using Eq.2, but Eq.2 generates higher values when $a/t > 0.6$. Therefore it is preferable to keep the ratio a/t within the range 0.4-0.6.

Although only porous NiO-YSZ material with 16% porosity was tested in this work, the current method of measuring K_{IC} should be also applicable to other brittle materials. The effect of notch shape and size on the measured K_{IC} value is discussed in detail in a separate paper [8]. The notch tip width in this work was 7.5±2.5 μm and the opening angle was smaller than 60˚ (Fig. 2a). According to the criteria given in [8], if the defect length at the notch tip is not significantly smaller than 7.5 μm, then the measured value of K_{IC} should be regarded as valid. The defect length in porous materials is not unambiguously defined, but can be regarded as a characteristic scale of the microstructure, which is approximately the sum of grain (or particle) size and pore size. In addition, the higher the porosity, the higher will be the probability that pores connect to form larger defects. In the present specimens having 16% porosity, it is likely that the porosity is interconnected and therefore not unreasonable to assume that the local defect size exceeds the notch width. This is consistent with the observed good consistency of the measured values of K_{IC} despite the possible variation notch tip radius from specimen to specimen.

If the method is applied to dense polycrystalline materials then the local defect size is approximately the grain size and for accurate measurement of K_{IC} the notch tip radius should be smaller than the grain size. When this method is applied to measure the toughness of amorphous or single crystal materials, for which local defect length at the notch tip cannot be anticipated or estimated, then care must be taken in the interpretation of the results. The limitation on specimen size mainly comes from the method of notch making and reliable load-displacement measurement. For very thin beams the notch could be made by ion-beam machining for example. However, in addition the beam thickness must be much greater than the local characteristic defect size otherwise the notch depth is not reliably defined.

Conclusions

1. A micro-mechanical test capable of measuring the Young's modulus and toughness of slender beam-shaped samples was designed, implemented and validated.
2. The compliance of a notched cantilever beam can be predicted using an analytical equation which can be used to check the test conditions or estimate the notch depth.
3. Two different equations for calculating K_{IC} show good numerical agreement for typical experimental parameters, especially when the ratio of notch depth to beam thickness is in the range 0.4-0.6. Hence the preferable notch depth for fracture toughness measurement should be about the half thickness of the beam.
4. The Young's modulus of porous NiO/YSZ anode support was measured as 139±4 GPa and K_{1C} as 2.13±0.27 MPa $m^{1/2}$.

Acknowledgements

This work was carried out as part of the project PROSOFC from the European Union's Seventh Framework Programme (FP7/2007-2013) for the Fuel Cells and Hydrogen Joint Undertaking under grant agreement number 325278.

References

[1] G. Delette, J. Laurencin, M. Dupeux, J.B. Doyer, Scripta Mater., 59 (2008) 31-34.
[2] B. Kuhn, F.J. Wetzel, J. Malzbender, R.W. Steinbrech, L. Singheiser, J. Power Sources, 193 (2009) 199-202.
[3] J. Malzbender, R.W. Steinbrech, L. Singheiser, J. Mater. Res., 18 (2003) 929-934.
[4] J. Kübler, ECF13, San Sebastian 2000, 2013.
[5] ASTM, ASTM, ASTM, West Conshohocken, PA, 2001.
[6] J. Kies, H. Smith, H. Romine, H. Bernstein, Fracture Toughness Testing and Its Applications, ASTM STP, 381 (1965) 328.
[7] B.F. Brown, C.D. Beachem, Corrosion Science, 5 (1965) 745-750.
[8] X. Wang, A. Atkinson, Journal of the European Ceramic Society, 35 (2015) 3713-3720.

Figure

Tables and Figures

Table 1

Sample	Length mm	Thickness mm	Width mm	E (resonance) GPa
Glass	28.8	0.5	6.44	72

Table 2.

Specimen	*a* (µm)	*L* (mm)	*t* (mm)	*ND* (mm)	* K_{IC} (MPa m$^{1/2}$)	**K_{1C} (MPa m$^{1/2}$)
1	94	2.05	0.33	0.95	2.04	1.88
2	140	3.1	0.33	0.90	2.21	2.19
3	202	3.25	0.33	0.75	2.29	2.40
4	230	2.85	0.33	2.15	1.62	1.72
5	80	3.95	0.35	0.5	2.26	1.96
6	164	3.25	0.31	0.75	2.01	2.06
7	158	2.15	0.33	1.35	2.38	2.40
8	176	2.55	0.33	0.95	2.49	2.55
9	202	2.14	0.32	1.36	1.88	1.97
Average					2.13±0.27	2.12±0.28

* Calculated using Eq.3, assuming $\nu = 0.3$

** Calculated using Eq.2

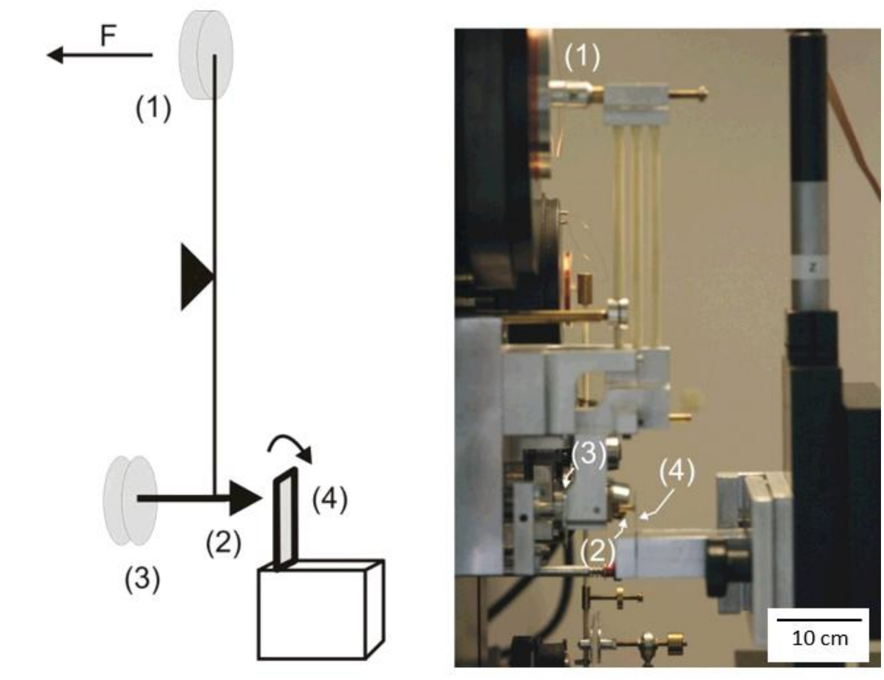

Fig. 1

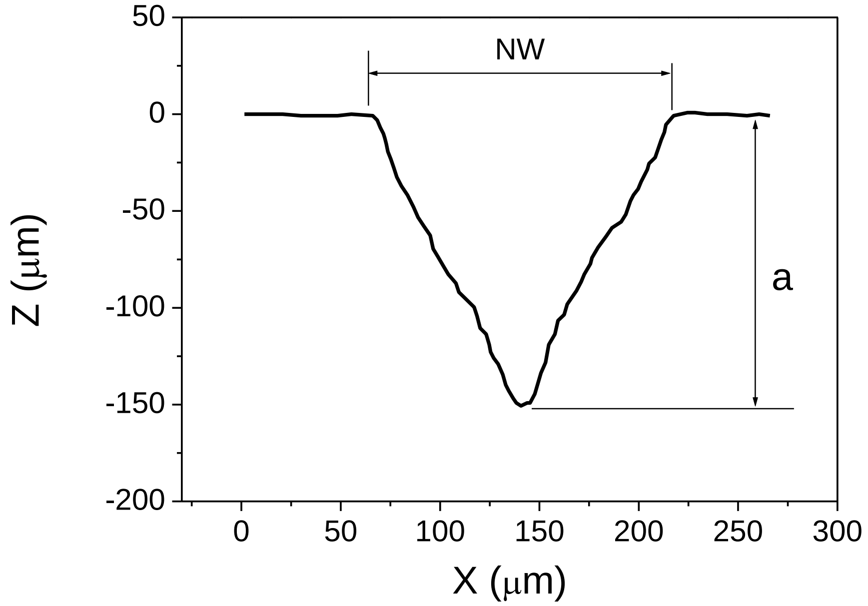

NW
a
Z (μm)
X (μm)
50
0
-50
-100
-150
-200
0
50
100
150
200
250
300

a)

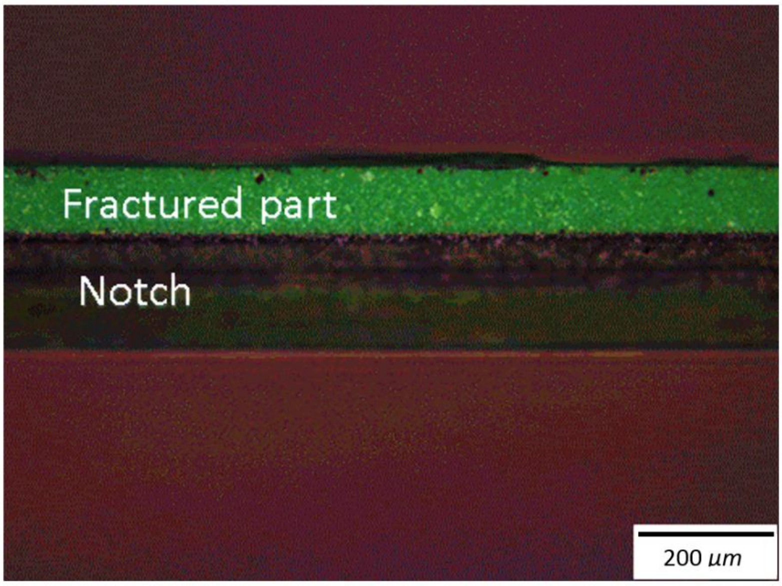

Fractured part
Notch
200 μm

b)

Fig. 2

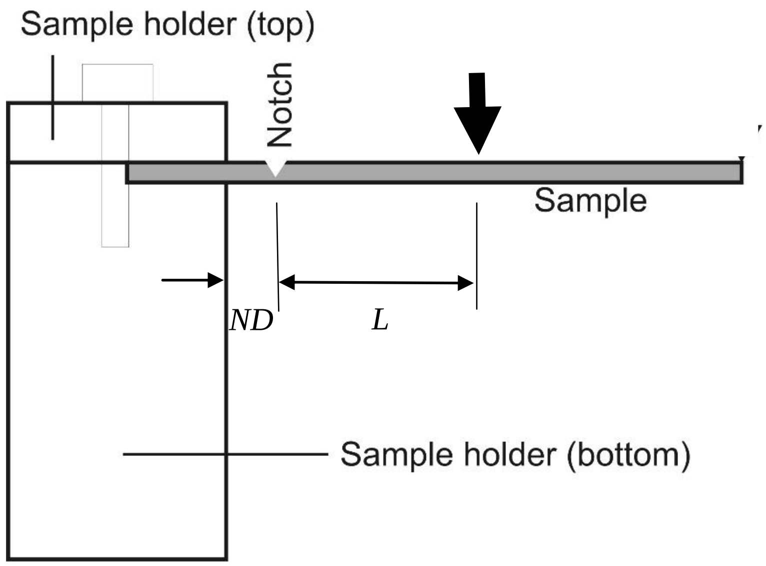

Fig. 3:

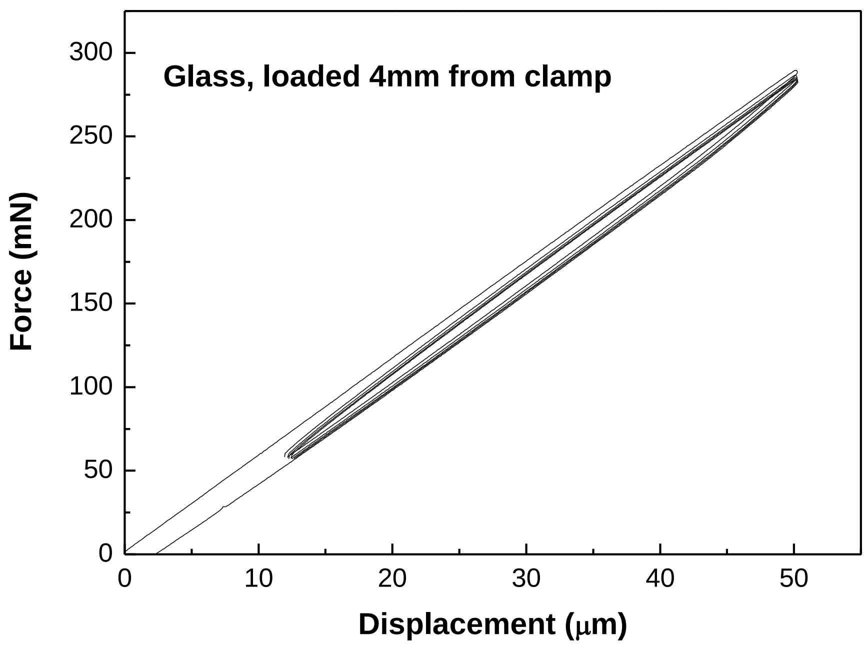
Glass, loaded 4mm from clamp
Force (mN)
Displacement (μm)
0
50
100
150
200
250
300
0
10
20
30
40
50

Fig. 4

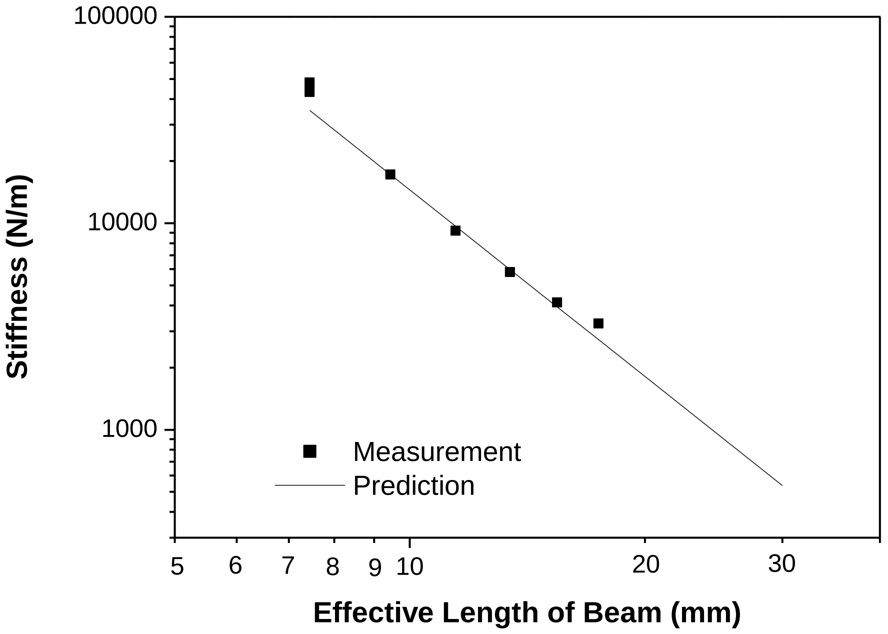
100000
10000
1000
Stiffness (N/m)
Measurement
Prediction
5
6
7
8
9
10
20
30
Effective Length of Beam (mm)

Fig. 5

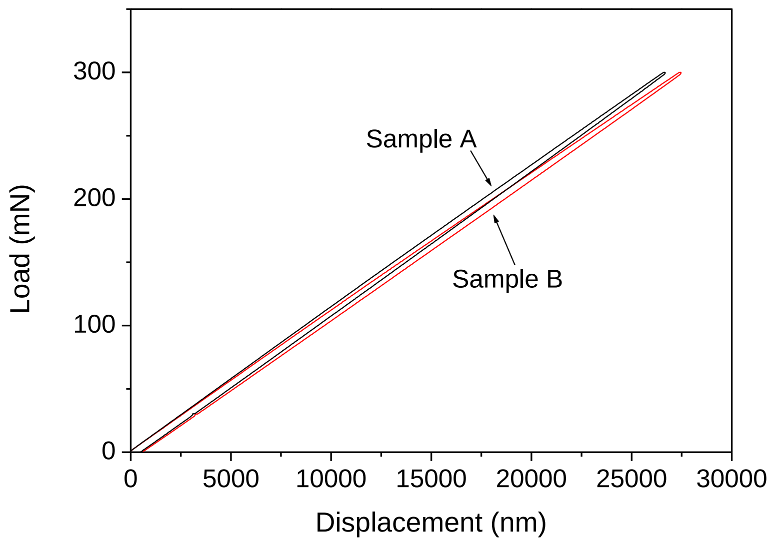

Load (mN)
300
200
100
0
0
5000
10000
15000
20000
25000
30000
Displacement (nm)
Sample A
Sample B

Fig. 6

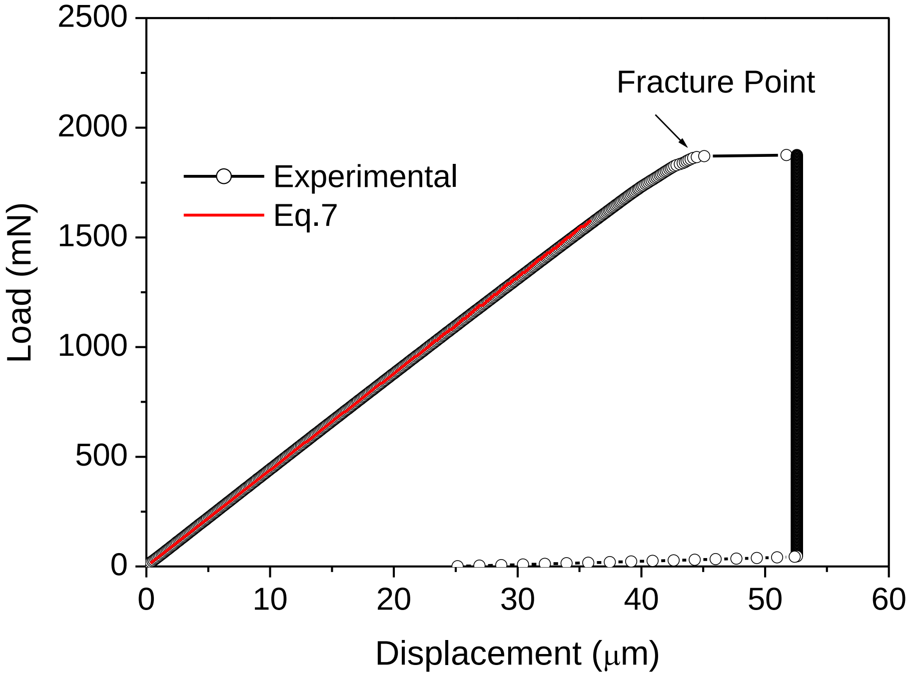

2500
2000
1500
1000
500
0
Load (mN)
0
10
20
30
40
50
60
Displacement (μm)
Fracture Point
Experimental
Eq.7

Fig. 7

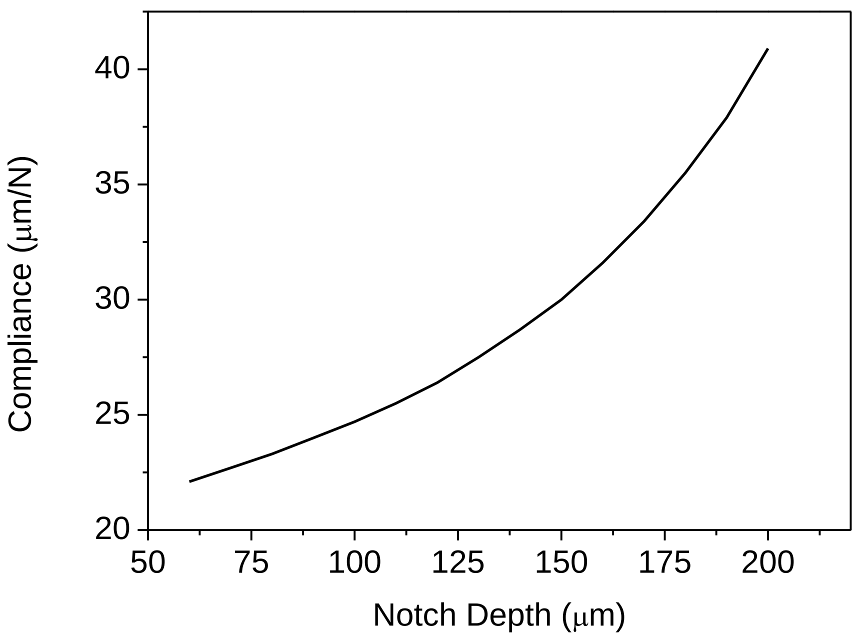
40
35
30
25
20
50
75
100
125
150
175
200
Compliance (μm/N)
Notch Depth (μm)

Fig. 8

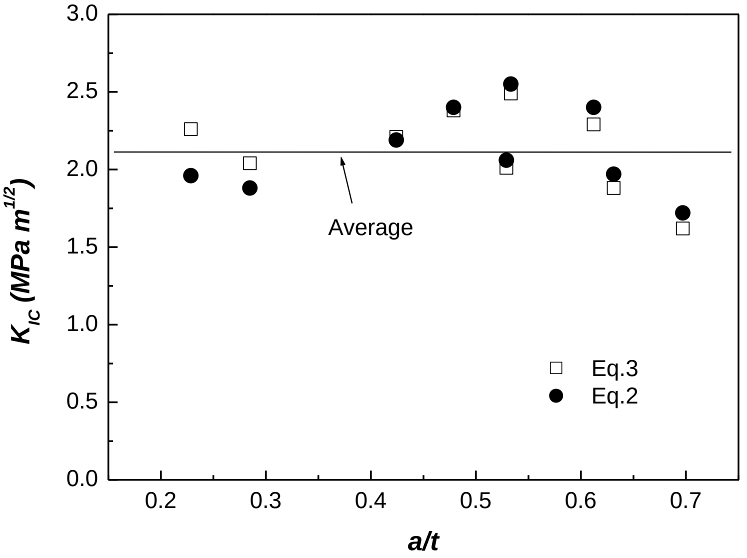

3.0
2.5
2.0
1.5
1.0
0.5
0.0
K_{Ic} (MPa m$^{1/2}$)
Average
Eq.3
Eq.2
0.2
0.3
0.4
0.5
0.6
0.7
a/t

Fig. 9

Captions

Table 1 Sample dimensions and elastic modulus of the glass validation samples.

Table 2. K_{IC} for NiO/YSZ SOFC anode supports obtained using different test conditions.

Fig. 1 Schematic and photograph of the Micro Materials nano- and micro-indenter (Micro Materials Ltd, Wrexham, UK) showing how the sample is fixed in place for the test to be carried out. (1) coil and magnet arrangement to apply a force to the pendulum, (2) indenter, (3) capacitive displacement sensor, (4) cantilever beam clamped in position for testing.

Fig. 2 a) A typical example of a notch profile; b) Notch depth determination by imaging on fractured cross section.

Fig. 3: Schematic of the sample clamping arrangement. The sample is clamped in a recess of 300 µm depth between a bottom and upper part of the clamp which is tightened using screws. *ND* is the distance from the clamping point to the notch and *L* the distance from the loading point to the notch.

Fig. 4 Load-displacement curves for the glass sample (un-notched) when being loaded 4 mm from its clamped end. The load was reduced to 20% of the maximum and then reloaded for 4 cycles before final unloading

Fig. 5 Stiffness of the glass sample as a function of the distance between the clamped end and the loading point compared with a prediction of the expected stiffness made using the independently determined value of the Young modulus.

Fig. 6 Loading and unloading curves for two NiO/YSZspecimens with nominally the same dimensions (20 mm by 3 mm by 0.33 mm) and $L = 7$ mm.

Fig. 7 Experimental load vs displacement curve, and theoretical prediction from Eq.7, for a test with $a = 0.080$ mm, $t = 0.33$ mm, $w = 3$ mm, $L = 3.95$ mm, $ND = 0.5$ mm.

Fig. 8 Predicted compliance as a function of notch depth for a beam with $t = 0.33$ mm, $w = 3$ mm, $L = 3.95$ mm, $ND = 0.5$ mm.

Fig. 9 Measured K_{IC} for NiO/YSZ SOFC anode supports as a function of relative notch depth a/t.